Environmental Science and Ecotechnology 21 (2024) 100440

Contents lists available at ScienceDirect

Environmental Science and Ecotechnology

journal homepage: www.journals.elsevier.com/environmental-science-and-ecotechnology/

Original Research

Optimizing anaerobic digestion: Benefits of mild temperature transition from thermophilic to mesophilic conditions

Xingxing Zhang [a], Pengbo Jiao [a], Yiwei Wang [a], Yinying Dai [a], Ming Zhang [a], Peng Wu [b, **], Liping Ma [a, c, *]

[a] Shanghai Key Lab for Urban Ecological Processes and Eco-Restoration, Shanghai Engineering Research Center of Biotransformation of Organic Solid Waste, School of Ecological and Environmental Sciences, East China Normal University, Shanghai, 200241, China
[b] School of Environmental Science and Engineering, Suzhou University of Science and Technology, Suzhou, 215009, China
[c] Technology Innovation Center for Land Spatial Eco-restoration in Metropolitan Area, Ministry of Natural Resources, Shanghai, 200062, China

ARTICLE INFO

Article history:
Received 6 December 2023
Received in revised form
9 June 2024
Accepted 10 June 2024

Keywords:
Temperature transition
Methane production
Cellular viability
Microbial community
Metagenomic binning

ABSTRACT

Anaerobic digestion (AD) plays a significant role in renewable energy recovery. Upgrading AD from thermophilic (50–57 °C) to mesophilic (30–38 °C) conditions to enhance process stability and reduce energy input remains challenging due to the high sensitivity of thermophilic microbiomes to temperature fluctuations. Here we compare the effects of two decreasing-temperature modes from 55 to 35 °C on cell viability, microbial dynamics, and interspecies interactions. A sharp transition (ST) is a one-step transition by 20 °C d^{-1}, while a mild transition (MT) is a stepwise transition by 1 °C d^{-1}. We find a greater decrease in methane production with ST (88.8%) compared to MT (38.9%) during the transition period. ST mode overproduced reactive oxygen species by 1.6-fold, increased membrane permeability by 2.2-fold, and downregulated microbial energy metabolism by 25.1%, leading to increased apoptosis of anaerobes by 1.9-fold and release of intracellular substances by 2.9-fold, further constraining methanogenesis. The higher (1.6 vs. 1.1 copies per *gyr*A) metabolic activity of acetate-dependent methanogenesis implied more efficient methane production in a steady mesophilic, MT-mediated system. Metagenomic binning and network analyses indicated that ST induced dysbiosis in keystone species and greatly enhanced microbial functional redundancy, causing loss of microbial syntrophic interactions and redundant metabolic pathways. In contrast, the greater microbial interconnections (average degrees 44.9 vs. 22.1) in MT at a steady mesophilic state suggested that MT could better maintain necessary system functionality and stability through microbial syntrophy or specialized pathways. Adopting MT to transform thermophilic digesters into mesophilic digesters is feasible and could potentially enhance the further optimization and broader application of practical anaerobic engineering.

1. Introduction

Microbially driven anaerobic digestion (AD) is a long-established technology adopted for methane (CH_4) production from a variety of organic waste types, including waste-activated sludge (WAS), food waste (FW), and livestock manure, thus facilitating sustainable waste management [1]. The efficiency of AD is primarily dictated by such operational parameters as temperature, solid retention time (SRT), organic loading rate (OLR), and pH [2]. Temperature can play a critical role in determining the performance and stability of AD by shaping microbial ecosystems, regulating metabolic activity, affecting cell physiology, and mediating enzyme biosynthesis [3,4]. Mesophilic (30–38 °C) and thermophilic (50–57 °C) temperatures are commonly used in industrial-scale biorefineries [5]. Most digesters are operated at mesophilic temperatures because doing so enables a more stable and less complex process with lower sensitivity to toxic inhibitors [6]. However, thermophilic digestion has increasingly gained attention, primarily due to its faster kinetics and better

* Corresponding author. Shanghai Key Lab for Urban Ecological Processes and Eco-Restoration, Shanghai Engineering Research Center of Biotransformation of Organic Solid Waste, School of Ecological and Environmental Sciences, East China Normal University, Shanghai, 200241, China.
** Corresponding author.
E-mail addresses: wupengniu@126.com (P. Wu), lpma@des.ecnu.edu.cn (L. Ma).

https://doi.org/10.1016/j.ese.2024.100440

performance for the same SRT [7]. Hence, driven by higher treatment capacity and CH_4 recovery efficiency, thermophilic digestion has increasingly been applied, particularly in treating recalcitrant wastes [8,9]. Nevertheless, thermophilic AD has possible disadvantages, such as an unpleasant odor, reduced digestate dewaterability, higher process instability, and higher heating requirements, which may offset its higher biogas production relative to mesophilic AD [10]. To alleviate these limitations, converting the thermophilic condition to the mesophilic condition is an alternative option that facilitates the sustainability of AD practices in regions with moderate or low temperatures and addresses the substrate shortage [11,12]. Two strategies are commonly adopted to shift to the designed temperature in AD systems: the use of a sharp transition (ST; one-step transition) and the use of a mild transition (MT; stepwise transition) [7,13]. Accordingly, it is important to elucidate the effects of the optional temperature shift strategies (ST/MT) on performance transitioning from thermophilic to mesophilic systems and identify which strategy best maintains system stability and efficiency. This determination would hold significant engineering importance.

The physiological status of microbial cells can be damaged when exposed to inhibitors (e.g., capsaicin, microplastics, and antibiotics) and adverse metabolic conditions (e.g., temperature and pH changes) [2,14]. In these scenarios, cell membrane integrity and microbial viability would be reduced, intracellular substances would be released, and cell energy metabolism would be downregulated, resulting in poor biogas production [15]. Thus, identifying the cellular functional state, intracellular substance release, and energy metabolism level can reflect the physiological responses of microbial cells to environmental stressors. In addition, oxidative stress, a common result of exposure to unfavorable conditions (i.e., low temperatures), could induce microbial reactive oxygen species (ROS) generation in anaerobic bioreactors [16,17]. The appropriate ROS level can stimulate cellular activity, but ROS overproduction can destroy cell integrity and increase membrane permeability [18]. Therefore, determining the ROS levels induced by a temperature shift is significant. Very little relevant information has emerged regarding temperature-transited thermophilic systems, especially under ST and MT strategies.

Quite a few studies have examined the effects of temperature shift on AD microbial dynamics [2,19]. For instance, a decrease in temperature from 37 to 25 °C was found to increase the abundance of Proteobacteria in cattle manure digesters [20], while Ruminococcaceae and *Methanobacterium* were found to be the main drivers of digester resilience to abrupt temperature disturbances from 55 to 35 °C [19]. Nonetheless, the effects of the ST and MT strategies on microbial dynamics, functional traits, and interactions in transitioning from thermophilic to mesophilic systems are poorly understood. Thermophilic and mesophilic conditions shape individual microbial consortia for CH_4 production, whereas thermophiles have been observed in mesophilic consortia, mesophiles cannot survive in thermophilic consortia [21]. Thus, rapid acclimation and colonization of mesophiles are necessary to maintain a balanced microbial trophic group among syntrophic bacteria and methanogenic archaea during the transition from thermophilic to mesophilic conditions. Community self-assembly and stabilization are fundamental to well-functioning AD systems, and the adaptation of microbial species is inherently driven by interspecies competitive and/or cooperative trophic interactions [22,23]. Therefore, high-resolution microbial community ecology and functionally core microbiome analyses, with further interpretations of essential interspecies interaction mechanisms, would be instrumental for engineering practices.

In this study, ST (one-step transition by 20 °C d^{-1}) and MT (stepwise transition by 1 °C d^{-1}) strategies for changing from thermophilic to mesophilic conditions are investigated for the anaerobic co-digestion (AcoD) of WAS with FW to reveal the physiological and microbial mechanisms of anaerobic microbiota in response to the temperature transition. Physiological responses related to cell integrity, oxidative stress, and enzyme content are examined. The dynamics, functional traits, and interspecies trophic-level networks of anaerobic consortia during the temperature shift are explored. Overall, we aim to elucidate microbial interactions and functions in anaerobic microcosms and to reveal key mechanisms that affect the stability of temperature-dependent AD processes.

2. Materials and methods

2.1. Reactor construction and operational strategies

Two thermophilic (55 ± 2 °C) anaerobic digesters (termed ST and MT) treating WAS and FW were constructed using continuous-stirred tank reactors, each with an effective volume of 6.0 L continuously stirred at 80 rpm by a paddle agitator (Supplementary Material Fig. S1). The WAS from the secondary settler of a wastewater treatment plant (treatment capacity 138,000 m^3 d^{-1}) (Shanghai, China) and mesophilic digested sludge from an industrial-scale anaerobic digester treating paper wastewater were mixed to initiate the reactors. The feedstock was prepared by mixing WAS and FW in a volatile solid (VS) ratio of 5:1. The FW (mainly containing noodles, rice, vegetables, and meat) was collected from a student canteen and homogenized after the removal of impurities (i.e., plastics, eggshells, and bones). Their basic characteristics are detailed in Table 1. The ratio of inoculum to feedstock was 3.5:1 (VS basis).

A semicontinuous operation was performed for each reactor by feeding and discharging once daily. The SRT and OLR of each reactor were maintained at 20 days and 2.6 ± 0.2 g VS L^{-1} d^{-1}, respectively. The operation continued for 176 days and was categorized into five phases according to different temperature transition strategies. Specifically, two reactors were operated at thermophilic (55 ± 2 °C) conditions in phase 1 (days 1–71) (Supplementary Material Table S1). The strategies were employed in phase 2 (days 72–91). The first involved a one-step temperature decrease from 55 to 35 °C directly for ST, and the second consisted of a stepwise temperature decrease from 55 to 35 °C in a decrement of 1 °C d^{-1} for MT. Each temperature decrease was conducted once per 24 h. After the temperature transition, both reactors were operated at mesophilic (35 ± 2 °C) conditions throughout the subsequent operation and showed acidification in phase 3 (days 92–101). Adding alkaline chemicals (i.e., NaOH) is an effective approach to regulating system pH and relieving acid inhibition, thereby enhancing the metabolic activity of methanogens. Considering the high sensitivity of functional microorganisms (i.e., acetogens and methanogens) to acidic pH [24], the pH was controlled within the range of 6.8–7.5 via the addition of 4 M HCl and/or 4 M NaOH in phase 4 (days 102–145) to provide a suitable pH environment. Specifically, a certain amount of 4 M NaOH was added to the reactors after each feeding operation during the initial period of phase 4 to gradually restore the pH to the range of 6.8–7.5. Afterwards, small amounts of 4 M HCl and/or 4 M NaOH were added after each feeding operation to maintain this pH range. The pH modification might have masked temperature-shift effects in subsequent restoration and stable mesophilic processes owing to its strong correlation with the overall state of the digesters [24]. Nonetheless, information on the temperature transition-related performance and underlying mechanisms could be obtained from the results of phases 1–3, and the ability of the reactor recovery and pH control to resist adverse effects of the temperature shift are the central issues of this study. Finally, two

Table 1
Characteristics of WAS, FW, feedstock, and inoculum used in this study.

Parameters (unit)	WAS	FW	Feedstock	Inoculum
pH	7.12 ± 0.13	5.83 ± 0.38	6.87 ± 0.23	7.43 ± 0.05
TS (g L^{-1})	26.36 ± 0.24	175.7 ± 0.56	60.67 ± 0.34	21.14 ± 0.21
VS (g L^{-1})	13.64 ± 0.16	167.2 ± 0.32	51.08 ± 0.25	15.63 ± 0.16
TCOD (g L^{-1})	13.58 ± 0.87	258.7 ± 4.85	92.33 ± 1.87	10.5 ± 0.14
SCOD (g L^{-1})	0.06 ± 0.01	86.7 ± 1.74	20.17 ± 0.74	0.04 ± 0.01
Total carbohydrates (g L^{-1})	0.23 ± 0.04	121.8 ± 2.17	37.54 ± 0.69	0.47 ± 0.02
Soluble carbohydrates (g L^{-1})	0.01 ± 0.00	70.58 ± 3.24	19.43 ± 0.23	0.01 ± 0.00
Total proteins (g L^{-1})	1.14 ± 0.08	52.12 ± 0.67	12.49 ± 0.34	1.25 ± 0.04
Soluble proteins (g L^{-1})	0.04 ± 0.00	24.29 ± 0.14	8.47 ± 0.26	0.03 ± 0.00
NH_4^+-N (mg L^{-1})	2.63 ± 0.02	251.7 ± 1.97	55.54 ± 0.87	27.74 ± 0.31
TA (mg $CaCO_3$ L^{-1})	346.5 ± 7.47	312.5 ± 10.4	321.5 ± 6.44	212.6 ± 1.32
TVFAs (mg COD L^{-1})	46.17 ± 0.57	1876.4 ± 20.9	946.28 ± 6.97	86.79 ± 0.42
C/N ratio	4.89 ± 0.23	13.17 ± 0.19	10.47 ± 0.28	5.12 ± 0.17
BMP (mL CH_4 per g VS_{fed})	69.31 ± 2.24	589.5 ± 6.45	412.4 ± 3.62	-

Note:
1 The data are expressed as mean value ± standard deviation ($n \geq 3$).
2 WAS, waste-activated sludge; FW, food waste; TS, total solid; VS, volatile solid; TCOD, total chemical oxygen demand; SCOD, soluble chemical oxygen demand; NH_4^+-N, ammonia; TA, total alkalinity; TVFAs, total volatile fatty acids; C/N, carbon to nitrogen; BMP, biochemical methane potential.

reactors operated stably in phase 5 (days 146–176). The long-term performance of the reactors was monitored according to the important operating parameters, including solid reduction efficiency (SRE), free ammonia nitrogen (FAN), and organic conversion efficiency (measurements are detailed in Supplementary Texts S1–S3).

2.2. Evaluation of oxidative stress, cell viability, and enzyme content

To evaluate the oxidative stress of cells affected by temperature transition, the ROS level and ROS-scavenging antioxidase activities, such as catalase (CAT), glutathione reductase (GR), and superoxide dismutase (SOD), were monitored. The adenosine 5′-triphosphate (ATP) content was assayed to reflect the microbial energy metabolism level. The damage proportion of anaerobes was measured using flow cytometry to assess cell viability. The lactate dehydrogenase (LDH) release was monitored to reveal membrane integrity. The enzyme activities of α-glucosidase (α-Glu), protease (PT), butyrate kinase (BK), acetate kinase (AK), carbon monoxide dehydrogenase (CODH), and coenzyme F_{420} were detected to elucidate the protein responses of the microbiome. To reveal the maintenance of microbial structural integrity, three layers of extracellular polymeric substances (EPS) — that is, slime EPS, loosely bound EPS (LB-EPS), and tightly bound EPS (TB-EPS) — were extracted using the modified heating method [15]. The composition and structure of the EPS fractions were characterized by three-dimensional excitation emission matrix spectroscopy (3D-EEM) and Fourier transform infrared spectroscopy. The fluorescent parameters, including the fluorescence index (FI), humification index (HIX), and biological index (BIX), were calculated using established methods [25]. In brief, the ratio between the fluorescence intensity at 470 and 520 nm with an excitation wavelength of 370 nm represented FI ($I_{470/520}$). The ratio between the area of 435–480 nm (A_4) and the sum area of 300–345 nm (A_1) and 435–480 nm (A_4) with an excitation wavelength of 254 nm represented HIX ($A_4/(A_1 + A_4)$). The ratio between the fluorescence intensity at 380 and 430 nm with an excitation wavelength of 310 nm represented BIX ($I_{380/430}$). Detailed EPS extraction and characterization procedures are presented in Supplementary Text S4.

2.3. DNA sequencing and bioinformatics analyses

To further identify the microbial communities and functional traits during the temperature shift, digestate samples ($n = 44$) in each phase were collected from two reactors (sampling information is presented in Supplementary Material Table S2) for DNA extraction using the FastDNA SPIN Kit for Soil (MP Biomedicals, USA). For microbial composition characterization, 44 extracted DNA samples were used for 16S rRNA gene amplicon sequencing with universal primers 515F (5′-GTGCCAGCMGCCGCGG-3′) and 806R (5′-GACTACHVGGGTWTCTAAT-3′) targeting the V4 region [26]. The detailed procedure of 16S high-throughput sequencing and downstream bioinformatics analyses of the microbial community are provided in Supplementary Text S5. For microbial function identification, 30 DNA samples were used for metagenomic sequencing using the Illumina Novaseq6000 platform, generating a total of 430 Gb metagenomic data. Metagenome-assembled genomes (MAGs) were retrieved from metagenomic reads and annotated using KEGG GhostKOALA, eggNOG 5.0, dbCAN2, and METABOLIC (v4.0) [26]. The metabolic functional pathways of the MAGs were synthetized by combining the genes and pathway results annotated by the above tools. The MAG retrieval and functional annotation procedures are detailed in Supplementary Text S6. The raw 16S and metagenomic datasets were deposited into the NCBI SRA database with Bioproject ID PRJNA942036 and PRJNA945358, respectively.

2.4. Reverse transcriptase quantitative PCR analysis

The transcriptional expression levels of acidogenesis-, acetogenesis-, and methanogenesis-related genes, which encoded AK (EC: 2.7.2.1), formyl tetrahydrofolate synthetase (FTHFS, EC: 6.3.4.3), acetyl-coenzyme A synthase (ACAS, EC: 6.2.1.1), and methyl coenzyme reductase (*mcr*A, EC: 2.8.4.1), were validated using reverse transcriptase quantitative polymerase chain reaction (RT-qPCR). The RT-qPCR results were normalized against the abundance of the housekeeping gene *gyr*A (DNA gyrase subunit A) [27]. The RNA extraction, cDNA synthesis, primer sequences, operational procedures, and annealing temperatures for the RT-qPCR assays are detailed in Supplementary Materials Text S7 and Table S3.

2.5. Other analytical methods

Total solid (TS), VS, chemical oxygen demand (COD), total alkalinity (TA), and ammonia (NH_4^+-N) concentrations were measured at an interval of 2–3 days using established methods [27]. The pH, oxidation–reduction potential (ORP), protein (PN), polysaccharide (PS), elemental composition, volatile fatty acid

(VFA) concentration, and biogas composition were detected following a previous study [28]. Flow cytometry determined microbial viability using an Annexin V-FITC apoptosis assay kit (Absin Biotechnology, Shanghai, China). Briefly, 10 mL of mixture samples were centrifuged at 3000 rpm for 5 min, and the pellets were resuspended in precooled sodium phosphate buffer (SPB, pH 7.4, 100 mmol L^{-1}). The suspension was then heated at 60 °C in a water bath for 30 min and resuspended using pre-cooled SPB. After filtering the suspension using a 40-μm strainer (Falcon, USA) and staining, the samples were determined using a BD Biosciences Accuri™ C6 Plus flow cytometer using the staining process mentioned in Supplementary Text S8. ROS, ATP, and LDH levels were detected using commercial ROS, ATP, and LDH double antibody sandwich enzyme-linked immunosorbent assay (ELISA) kits. Briefly, the mixture samples were centrifuged at 5000 rpm for 10 min, and the 50 μL supernatants from each sample were used for the measurements. After adding four reagents in order, the absorbance was monitored at 450 nm using a microplate, and the concentrations of ROS, ATP, and LDH were calculated according to the standard curve. ELISA kits were also used to determine enzyme activity. Briefly, the collected samples were washed repeatedly and resuspended using SPB (pH 7.4, 100 mmol L^{-1}), sonicated at 20 kHz and 4 °C for 30 min to destroy microbial cells, and then centrifuged at 10,000 rpm and 4 °C for 15 min to obtain the cell extracts. The extracts were kept cold on ice before analysis. The measurements of ROS, ATP, LDH, CAT, GR, SOD, α-Glu, PT, BK, AK, CODH, and coenzyme F_{420} are detailed in Supplementary Texts S9–S11.

2.6. Statistical analysis

Significance analysis of the data was conducted via a one-way ANOVA test with an LSD posthoc comparison in IBM SPSS Statistics v27.0 software, and $p < 0.05$ was considered statistically significant. A bubble plot was made to show the abundance of microbial genera using the online tool ChiPlot (https://www.chiplot.online/), and a heat map plot showing the abundance of MAGs was created in R (v4.2.2) with the *pheatmap* package. The principal coordinates analysis (PCoA), microbial biodiversity, and redundancy analysis (RDA) of the samples were implemented using the R *Vegan* package. The candidate biomarkers among the different phases were identified by linear discriminant analysis effect size (LEfSe) analysis [2]. A nonparametric factorial Kruskal–Wallis sum-rank test was performed with a significance level of $p < 0.05$, and the threshold value of the logarithmic linear discriminant analysis (LDA) score was 2.0 [29]. The ecological interactions of the MAGs in the microbiomes were explored using the R *Hmisc* and *igraph* packages. Network analysis was based on the pairwise Spearman's rank correlations (r) between the MAGs, and only robust ($r > 0.6$) and statistically significant ($p < 0.01$) correlations were considered. Cooccurrence network visualization and topological properties were attained with Gephi (v0.10.1).

3. Results and discussion

3.1. Digester performance deterioration and recovery

Two thermophilic digesters were successfully started within 25 days in phase 1 (days 1–71), after which the performance of the digesters was stable and comparable ($p > 0.05$) across more than two HRT operations (Fig. 1a). The subsequent implementation of the ST strategy immediately caused dramatic decreases in the methane production rate (MPR) and SRE during phase 2 (days 72–91). Similarly, Sudiartha et al. reported a 33% reduction in CH_4 production during glucose digestion after a rapid temperature drop from 55 to 45 °C [30]. Madigou et al. observed the termination of biogas production during the AD of cellulose when the temperature was shifted from 55 to 35 °C via the ST strategy [19]. Although the MPR showed a substantial increase on days 72–77 due to the persistence of the large quantity of methanogenic enzymes from phase 1 [19], it constantly decreased to 151.2 mL CH_4 L^{-1} d^{-1} via the ST strategy at the end of phase 2. By contrast, MPR and SRE undulated in the ranges of 825.5–1455 mL CH_4 L^{-1} d^{-1} and 71.2–77.2% via MT, respectively, which were significantly higher than those via ST (151.2–1197 mL CH_4 L^{-1} d^{-1} and 60.4–75.5%, respectively) ($p < 0.05$), indicating that MT could sustain relatively higher stable and efficient AD against ST during the transition period. The difference in performance deterioration between ST and MT was also indicated in the process parameters (e.g., pH, ORP, FAN, TA, and total VFAs (TVFAs)/TA ratio) (Supplementary Material Fig. S2). Previous studies found that the transition from 37 to 25 °C via the ST strategy significantly decreased MPR and increased TVFA concentrations, which could be attributed to the faster adaptation of acidogens or a greater temperature span of acidogens at lower temperatures compared to methanogens, as methanogens typically exhibit slower growth and have a narrower temperature span [20,29].

The reactors were then operated under mesophilic conditions in phases 3–5. ST reached an acidified state in phase 3 (days 92–101), while MT was slightly acidified (Table 2). PH adjustment was adopted in phase 4 (days 102–143) to recover reactors. It was observed that MT recovered much faster than ST, as indicated by MT reaching a new steady state (MPR 1391 ± 50.5 mL CH_4 L^{-1} d^{-1}) in 22 days, whereas ST reached a new steady state (MPR 1552 ± 26.9 mL CH_4 L^{-1} d^{-1}) within 39 days. This demonstrates that pH adjustment within an optimal range (6.8–7.5) can promote the recruitment of acid-degrading and methanogenic microbes [24,31] and that pH adjustment is thus a practical solution for tackling the acidification of mesophilic co-digestion of WAS with FW. Previous studies have demonstrated that controlling pH by adding NaOH solution improves the buffering capacity of the system, effectively preventing acid inhibition and recovering collapsed systems [32,33]. Nevertheless, the inhibition of microbial activity by high ion (Na^+) concentrations should be avoided. The faster performance recovery in MT might be related to the active ecological roles of microbial immigrants in the digester [34]. During the steady state of phase 5 (days 144–176), MT (MPR 1345 ± 20.8 mL CH_4 L^{-1} d^{-1}, SRE 70.2 ± 3.6%) significantly outperformed ST ($p < 0.05$) (MPR 1129 ± 31.3 mL CH_4 L^{-1} d^{-1}, SRE 67.4 ± 2.9%). The better CH_4 production performance in MT is partially explained by the efficient utilization of intermediates by VFA oxidizers and methanogenic archaea [6], as the TVFA concentration in MT (83.3 ± 11.7 mg COD L^{-1}) was significantly lower than that in ST (228.3 ± 32.4 mg COD L^{-1}) ($p < 0.05$). This study demonstrated that MT is preferable for anaerobic digesters transferring from thermophilic to mesophilic conditions. It enables more robust and efficient operation and faster recovery regarding CH_4 production and VS reduction.

3.2. Physiological mechanism of performance affected by ST and MT

3.2.1. ST released more intracellular organic matter than MT

LB-EPS and TB-EPS were extracted to reveal the EPS variations and cell decomposition. EPS is a high-molecular polymer secreted by microbes as a protective barrier against microbial risks from environmental stressors [15]. The soluble PN concentrations in the LB-EPS and TB-EPS decreased significantly ($p < 0.05$) in both ST and MT during phases 2 and 3 (Fig. 1b), while the soluble PS concentration slightly decreased, indicating that more intracellular substrates were released from microorganisms after temperature shifts [35]. A 3D-EEM analysis of the major components in EPS also elucidated the substantial decrease of soluble PN and PS, reflecting

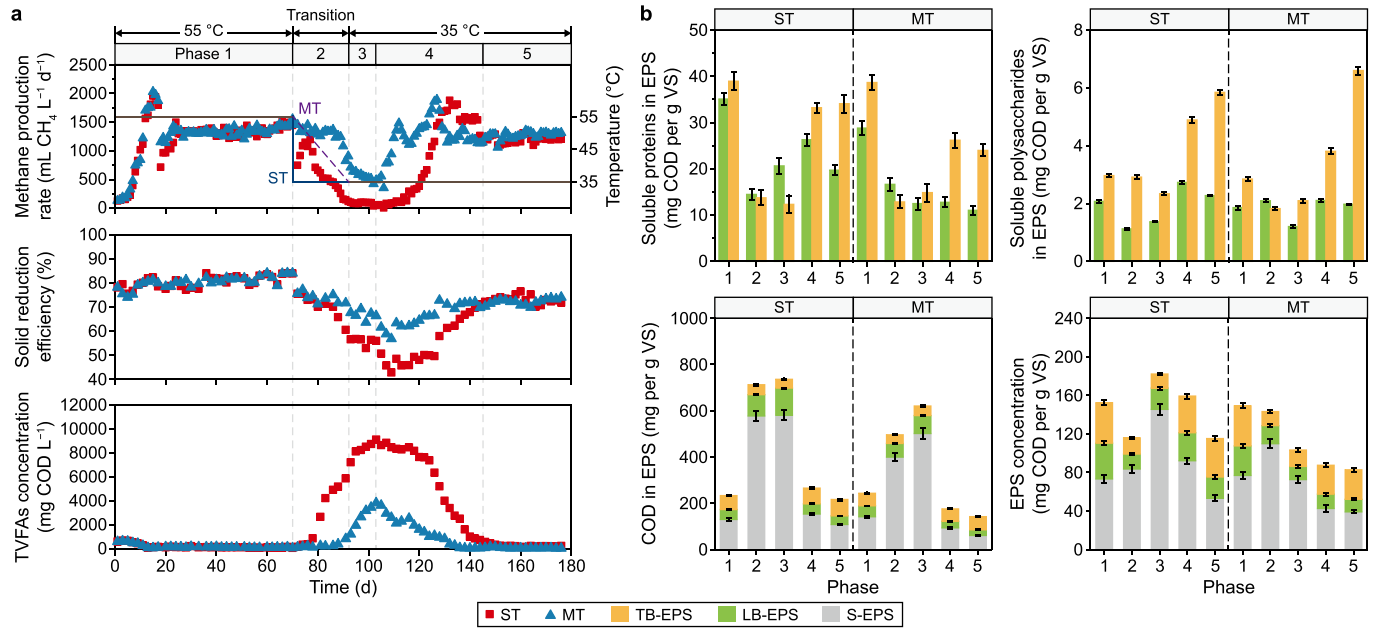

Fig. 1. Long-term performance of the two digesters. **a**, Methanogenesis performance regarding methane production rate, solid reduction efficiency, and TVFAs concentration. **b**, Composition and content of EPS fractions.

Table 2
Volatile fatty acid (VFA) concentrations in each phase of the reactors.

Reactor	ST			MT		
Concentration (mg COD L^{-1})	Acetate	Butyrate	Propionate	Acetate	Butyrate	Propionate
Phase 1	29.4 ± 10.7	7.7 ± 3.4	3.7 ± 4.5	30.6 ± 14.3	5.9 ± 4.7	5.1 ± 3.8
Phase 2*	2149.5	967.1	1204.4	386.7	86.2	159.4
Phase 3*	4265.3	936.4	2110.8	2064.4	285.9	649.8
Phase 4	329.5 ± 180.4	80.6 ± 50.4	149.7 ± 89.8	35.7 ± 20.8	14.8 ± 8.7	24.2 ± 19.4
Phase 5	121.4 ± 95.6	45.2 ± 33.5	75.5 ± 67.1	32.4 ± 25.7	12.6 ± 9.4	18.8 ± 14.6

Note:
1 The concentrations are denoted as mean value ± standard deviation ($n \geq 3$) during stable operation in each phase.
2 * represents the highest VFA concentration at acidified phases (phases 2 and 3) in the reactors.

that the fluorescence intensity scores of tryptophan/tyrosine aromatic protein−like substances and soluble microbial product−like substances showed a significant decrease during a temperature shift (Supplementary Materials Figs. S3−S4 and Tables S4−S5). Supplementary Material Fig. S3 also reveals several functional groups related to PS, PN, hydrocarbons, and nucleotides in the LB-EPS and TB-EPS (Supplementary Material Table S6), and the peak intensities of these groups appeared weak with ST and MT. This indicates the loss of major intracellular components due to cell lysis. Notably, the total COD of EPS in ST (711.8 ± 22.3 mg per g VS) was significantly greater ($p < 0.05$) than that in MT (495.7 ± 17.4 mg per g VS) in phase 2, demonstrating that ST induced more intracellular organic substances to release than MT (Supplementary Material Fig. S4).

Low temperatures generally stimulate microbes to produce more EPS to resist environmental stressors [36]. However, the EPS concentration of ST in phase 2 was 24.0% lower than in phase 1, owing to the collapse of the EPS-based defense system under such overwhelming temperature fluctuation conditions. Similarly, Li et al. observed a decrease in EPS secretion in anaerobic consortia as the temperature decreased from 35 to 10 °C [37], further revealing that the physical barrier generated by EPS in biological systems is limited under such stressful conditions. Intriguingly, the EPS concentration of the MT reactor consistently declined irrespective of the temperature drop because i) both thermophiles and mesophiles can tolerate and acclimate to a gentle temperature decrease such that they no longer secrete excessive EPS for microbial metabolism [7,38] and ii) cells may reduce the release of EPS from bound PN and PS at mesophilic temperatures (35 °C) compared with thermophilic temperatures (55 °C) [39]. Additionally, a high average FI value of 2.2 (above the microbial organic metabolic threshold of 1.9), together with the significant increments of BIX and HIX values, confirmed that the components of LB-EPS and TB-EPS were mainly derived from bacterial secretion rather than an exogenous source [40]. The increased intracellular release in ST enormously facilitated the conversion of the intracellular organics into VFAs and resulted in VFA accumulation due to the acid inhibition of methanogens [2].

3.2.2. *ST induced higher oxidative stress in anaerobes than MT*

The low ROS concentration maintained in normal anaerobes can mediate cellular signaling, but ROS overgeneration in anaerobes that encounter adverse environmental conditions (e.g., low temperature or high oxygen) can cause toxic oxidative stress and, thus, cellular injury [16,41]. The ROS generation via ST and MT strategies significantly increased ($p < 0.05$) to 1.6- and 1.4-fold of phase 1 (Fig. 2a), indicating that temperature shift — particularly the ST strategy — induced a high level of intracellular ROS production and remarkable cell pressure for environmentally sensitive

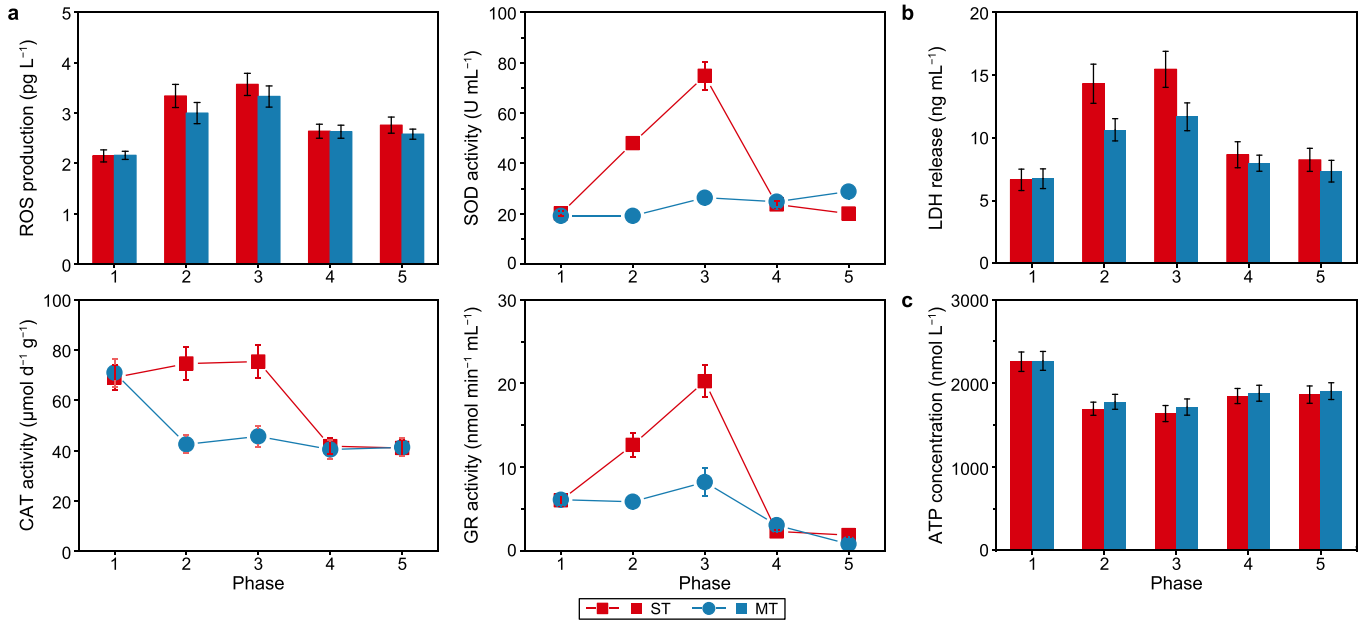

Fig. 2. Physiological status of microbial cells in ST and MT reactors. **a**, ROS production and activity of ROS-scavenging antioxidases, including superoxide dismutase (SOD), catalase (CAT), and glutathione reductase (GR). **b,** LDH release. **c,** ATP level.

thermophiles (Supplementary Material Fig. S5). The two primary reasons for ROS production by temperature drop may be (i) electron transport imbalance (i.e., electrons leaked from the electron transport chain were captured by molecular oxygen to form ROS [42]) and (ii) dissolved oxygen stress that originated from enhanced oxygen dissolution and decreased coexisting aerobe respiration [43]. The excessive ROS corresponding to enhanced oxidative stress would cause damage to intracellular DNA and protein [16,43], triggering an increase in the apoptosis of anaerobes and excessive release of intracellular substances as well as a decrease in the microbial metabolism activity (Fig. 2). Previous studies observed that the generation of ROS (e.g., hydrogen peroxide (H_2O_2)) in the scenario of the temperature decrease shock substantially confined the metabolic capacity, cell viability, and electron transfer activity of anaerobes [18,42], thereby significantly diminishing AD performance.

The critical ROS scavengers included SOD, CAT, and GR, which have been identified in many methanogenic archaea (*Methanobacterium* and *Methanosarcina*) [44], and interestingly, their activities exhibited significant divergences in response to ROS stress with ST and MT strategies (Fig. 2a—Supplementary Material Fig. S5). Specifically, the activities of antioxidases (SOD, CAT, and GR) were enhanced 1.1−2.4-fold with the ST strategy for coping with the increased oxidative stress by mesophilic conditions. This emphasizes the importance of enzymatic antioxidant defense mechanisms for obligate anaerobes (i.e., methanogenic archaea) to resist oxidative stress in reactors [45]. In contrast, the activities of antioxidases showed no obvious increase with MT, while CAT significantly decreased 1.7-fold ($p < 0.05$), indicating that H_2O_2 may be accumulated as the major ROS component. However, the overproduced ROS led to a significant decrease in the antioxidant capacity of cells after the temperature shift, which could cause the oxidative death of cells and an apparent debase in CH_4 production.

3.2.3. ST destroyed more cell integrity of microorganisms than MT

The performance and stability of anaerobes' metabolizing substrates were mainly determined by their cell physiological patterns [46,47]. The fluorescence percentage of early apoptotic cells indicated by Q3 and necrotic (or late apoptotic) cells indicated by Q2 in ST (9.9% and 5.9%, respectively) were higher than those in MT (7.5% and 3.3%, respectively) after a temperature shift (Supplementary Material Fig. S3). Therefore, the higher percentage of apoptotic cells (15.8% vs. 10.8%) and lower percentage of viable cells (i.e., Q4, 81.8% vs. 87.9%) in ST than in MT indicated that the sharp temperature transition resulted in a significant loss of cell viability (Supplementary Material Fig. S5). This result can be further supported by the LDH response of the anaerobes shown in Fig. 2b. Specifically, ST and MT in phase 2 obtained significant LDH increments to 2.2-fold and 1.6-fold those in phase 1 ($p < 0.05$), representing severe cytoderm and cytomembrane damage, particularly with ST. Thus, it could be inferred that a substantial increase in intracellular release with ST and MT was highly related to the destruction of the cytomembrane and early apoptosis of cells. The impaired viability of the microcosm in both ST and MT aligned with the observation of deteriorating CH_4 production performance in phase 2.

3.2.4. ST downregulated more cell energy metabolism levels than MT

The unfavorable effects of ST and MT on microbial metabolic activity were confirmed by determining ATP content, which was present in all living microorganisms and indicated microbial viability [48]. The ATP contents in ST and MT were decreased by 25.1% and 21.4%, respectively, in phase 2 compared to phase 1, and the reduction was further exacerbated during phase 3 (Fig. 2c). These observations revealed that a temperature drop suppressed the metabolic activities of most anaerobes, causing abnormal ATP synthesis and less bioenergy to complete methanogenic metabolism in high organic flux environments and the eventual termination of the reaction at acid-producing metabolism due to the preference of anaerobes to evolve short and incomplete pathways [23]. A previous study reported that electron transfer and oxidative phosphorylation were responsible for ATP synthesis in methanogenic bioreactors [49], while decreasing temperature may reduce the oxidative phosphorylation level and trigger electron leakage [42], leading to ATP diminution and even cytomembrane damage

due to an overload of potential differences.

In summary, temperature shifts negatively affected the cellular physiological and functional states of thermophilic microorganisms, particularly with ST. This was evident through the substantial increase in ROS concentration induced by ST, resulting in severe damage to cytomembrane permeability and integrity and a decline in microbial respiratory metabolism levels. This might explain the differences between ST and MT in cell apoptosis and intracellular release. The pH control (6.8−7.5) in phase 4 was effective in cellular metabolic recovery, which can be attributed to (i) neutral pH decreasing the concentration of undissociated VFAs and thus the toxicity of undissociated VFAs to cells [50]; (ii) pH regulation altering acid-producing metabolic pathways and preventing the overproduction of VFAs [24]; and (iii) a suitable pH potentially improving the metabolic activity of methanogens and maintaining a balance between acid-producing and methanogenic consortia [51]. This probably benefited the ROS of the ST and MT, which decreased to a normal level during stable operation, thereby reducing LDH release and improving ATP content, finally increasing the intact cells. Importantly, the superiority of MT performance over ST in phase 5 may be a consequence of discrepancies in overall oxidative stress, cellular integrity and viability, and microbial metabolic activity (Fig. 2). One convincing piece of evidence was that MT had a higher proportion of viable cells (89.3% vs. 82.0%) and a lower proportion of apoptotic cells (9.8% vs. 15.7%) compared with ST. This apparent difference confirmed the well-functioning mesophiles in MT. These findings elucidate the physiological mechanisms of microbial cells in response to temperature-shift stress.

3.3. Effects of ST and MT on individual step, key enzyme activity, and metabolic activity

To further understand the impacts of ST and MT on CH_4 production, the changes in the individual digestion step, the relevant enzyme activity, and encoded gene expression were monitored. Exploring the AD steps representing reaction processes, synergistic effects, and biodegradation kinetics could enhance our comprehension of the temperature transition effects on organic metabolism. After the ST shift, the percentages of hydrolysis, acidogenesis, acetogenesis, and methanogenesis decreased by 6.0%, 70.5%, 75.9%, and 76.4%, respectively (Supplementary Material Fig. S6). By contrast, the four steps displayed implicit reduction ($p > 0.05$) in MT in phase 2, thereby sustaining robust performance. A greater decrease in the ratio of hydrolysis, acidogenesis, acetogenesis, and methanogenesis via the ST strategy compared with the MT strategy could partially explain the slighter decrease in CH_4 production for MT (38.9%) relative to ST (88.8%) after the transition period. Notwithstanding, MT significantly lowered the ratios of the four steps in phase 3 ($p < 0.05$), thereby initiating methanation inhibition. These results are supported by enzyme- and gene-level evidence. Apart from PT, the activities of α-Glu, BK, AK, CODH, and coenzyme F_{420} were significantly inhibited by the ST strategy during phases 2 and 3 ($p < 0.05$) (Fig. 3a), indicating that ST caused conspicuous decreases in hydrolysis, acidogenesis, acetogenesis, and acetate-dependent methanogenesis. Interestingly, the PT activities during phase 2 in ST and MT were 27.8% and 33.1% higher, respectively, than those of phase 1, indicating that a temperature drop increased the capacity of hydrolyzers for the transformation of proteins into their microforms (e.g., amino acids). The enhanced proteolysis aligned with the increased abundance of proteolytic bacteria *Prevotella* via ST and MT strategies [52], which had a strong resistance to low-temperature disturbance [7,53]. However, the improved proteolysis could not compensate for the decreases in the overall hydrolysis capacity since an improvement in α-Glu activity was crucial for methanogenic substrate production during the AcoD of WAS with FW [54]. Consistent with the enzyme results, the gene expression levels of AK, FTHFS, ACAS, and methyl coenzyme reductase (*mcr*A) were significantly inhibited with ST ($p < 0.05$) (Fig. 3b and c). In particular, ACAS and *mcr*A in phase 2 were merely 13.0% and 16.1%, respectively, of those in phase 1 (Supplementary Material Fig. S6), denoting that acetate-dependent and all-pathway methanogenesis were the most susceptible to temperature variation. Numerous studies have emphasized the vulnerability of methanogens to environmental stressors, thus dramatically decreasing their abundance and microbial activities [1,3]. Although the gene expression levels of AK, FTHFS, ACAS, and *mcr*A declined significantly ($p < 0.05$) in MT during phase 2, such decline in MT was much lower than that in ST, revealing that the inhibition of ST to thermophilic AD was much more severe than that of MT during temperature transition.

The ratios of hydrolysis, acidogenesis, acetogenesis, and methanogenesis in ST and MT returned to normal levels and stabilized at 70.2−71.5%, 74.4−79.8%, 74.8−80.4%, and 74.4−79.9%, respectively, during phase 5. Other than hydrolysis, the ratios of acidogenesis, acetogenesis, and methanogenesis in MT were significantly higher ($p < 0.05$) than those in ST, which explained that MT showed better CH_4 production performance against ST. The shifts in key enzyme activity and functional gene expression in phase 5 also provided visual enzyme- and gene-level evidence for system recovery and better performance in MT. For instance, the CODH activity (35.9 ± 3.5 U L^{-1}) and ACAS gene expression (1.6 ± 0.1 copies per *gyr*A) in MT that reflected acetate-dependent methanogenesis were significantly greater than those in ST (32.6 ± 2.3 U L^{-1}, 1.1 ± 0.1 copies per *gyr*A), indicating that acetate-dependent methanogenesis, as the predominant methanogenic pathway in MT, conducted more efficient CH_4 production than that in ST.

3.4. Shift in microbial community and functional metabolism arising from ST and MT strategies

3.4.1. Microbial community assembly patterns

Temperature transition (both ST and MT) significantly increased community diversity, richness, and evenness (Supplementary Material Fig. S7). PCoA revealed that ST and MT caused a significant discrepancy in the predominant microbial community structure, while the reactors had analogous microbiota compositions during performance recovery and stable operation (Fig. 4a). There were large variations in the types and relative abundances of the predominant phyla and genera within the digesters in response to ST and MT (Fig. 4b and c). For instance, the predominant genera in phase 1 were S1 (56.6−79.5%) and SHD-231 (4.0−8.3%), but the predominant genera were shifted to *Prevotella* (6.0%), *Anaerobaculum* (5.3%), and SHD-231 (3.8%) in ST and *Treponema* (17.6%), *Streptococcus* (7.5%), *Anaerobaculum* (6.5%), and SHD-231 (5.2%) in MT at the end of phase 2. Meanwhile, *Methanothermobacter* (6.3% in ST, 6.1% in MT) and *Methanosarcina* (3.0% in ST, 6.1% in MT) flourished as the most predominant methanogens. Discrepant core microbes were selectively enriched due to the different temperature-shift strategies. These predominant populations varied significantly during acidified phase 3; for example, ST was dominated by *Megasphaera* (9.9%), *Prevotella* (9.7%), *Selenomonas* (9.2%), and RFN20 (4.2%), while MT was dominated by *Anaerobaculum* (6.1%), *Prevotella* (5.4%), *Treponema* (4.9%), and SHD-231 (3.9%). As mentioned earlier, the excessive ROS induced by the temperature transition caused a significant loss of relevant cell viability. It inhibited biomethanation processes, a pattern that would affect the microbial community succession relevant to these processes [17].

The discrepant functional genera were selectively enriched after performance recovery in phase 4. Specifically, *Aminobacterium*

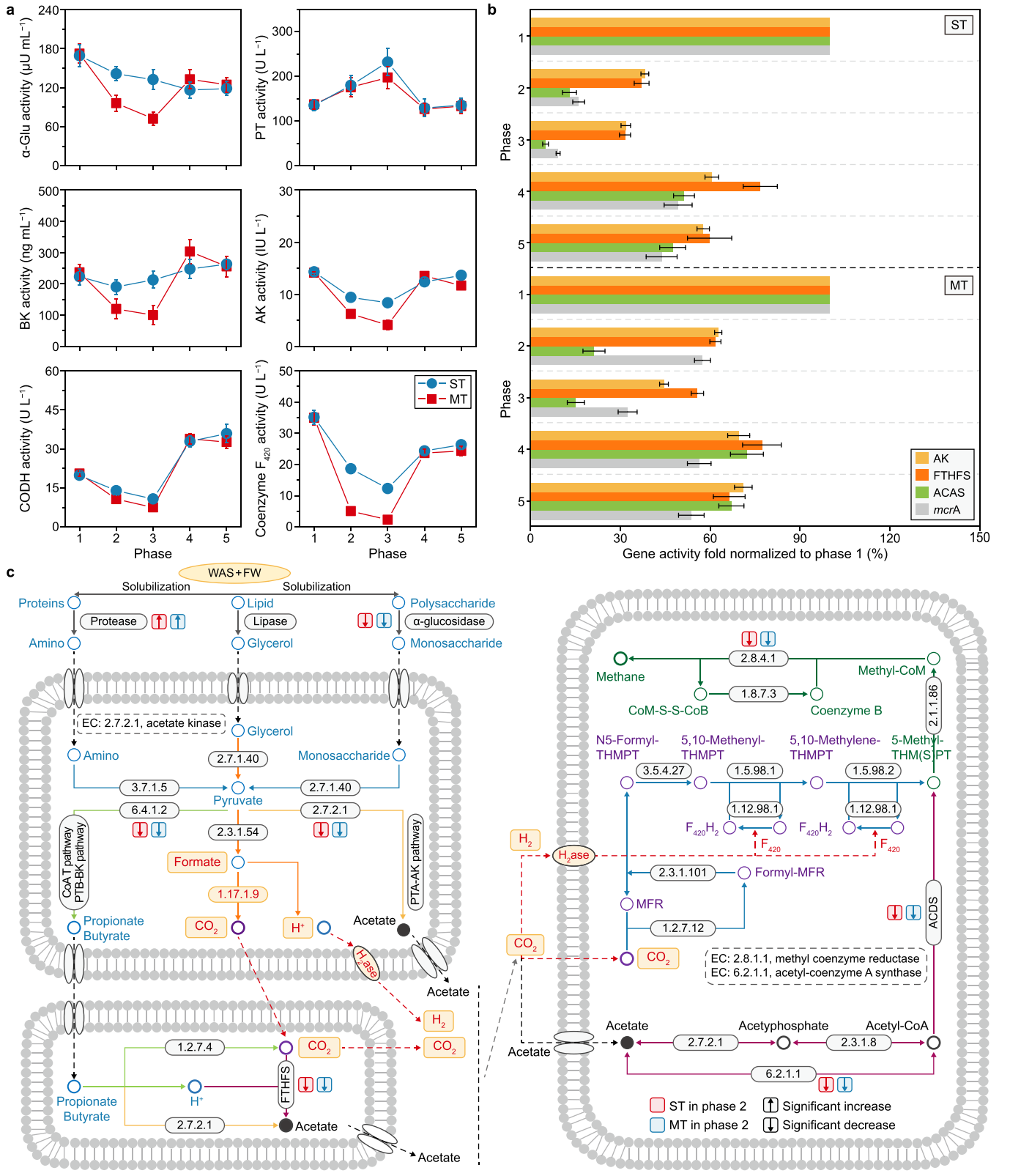

Fig. 3. Responses of key enzyme activity and gene expression of anaerobic microbes to temperature shift stress. **a**, The activities of α-glucosidase (α-Glu), protease (PT), butyrate kinase (BK), acetate kinase (AK), carbon monoxide dehydrogenase (CODH), and coenzyme F_{420}. **b,** RT-qPCR results targeting AD-related genes, including AK, formyl tetrahydrofolate synthetase (FTHFS), acetyl-coenzyme A synthase (ACAS), and methyl coenzyme reductase (*mcr*A). The number of mRNA transcripts was normalized against the number of *gyr*A mRNA transcripts, and data was present on the relative gene activity of phase 1. **c,** Schematic diagram of the response of metabolic pathways for CH_4 production in AcoD under temperature shift stress. WAS, waste-activated sludge; FW, food waste.

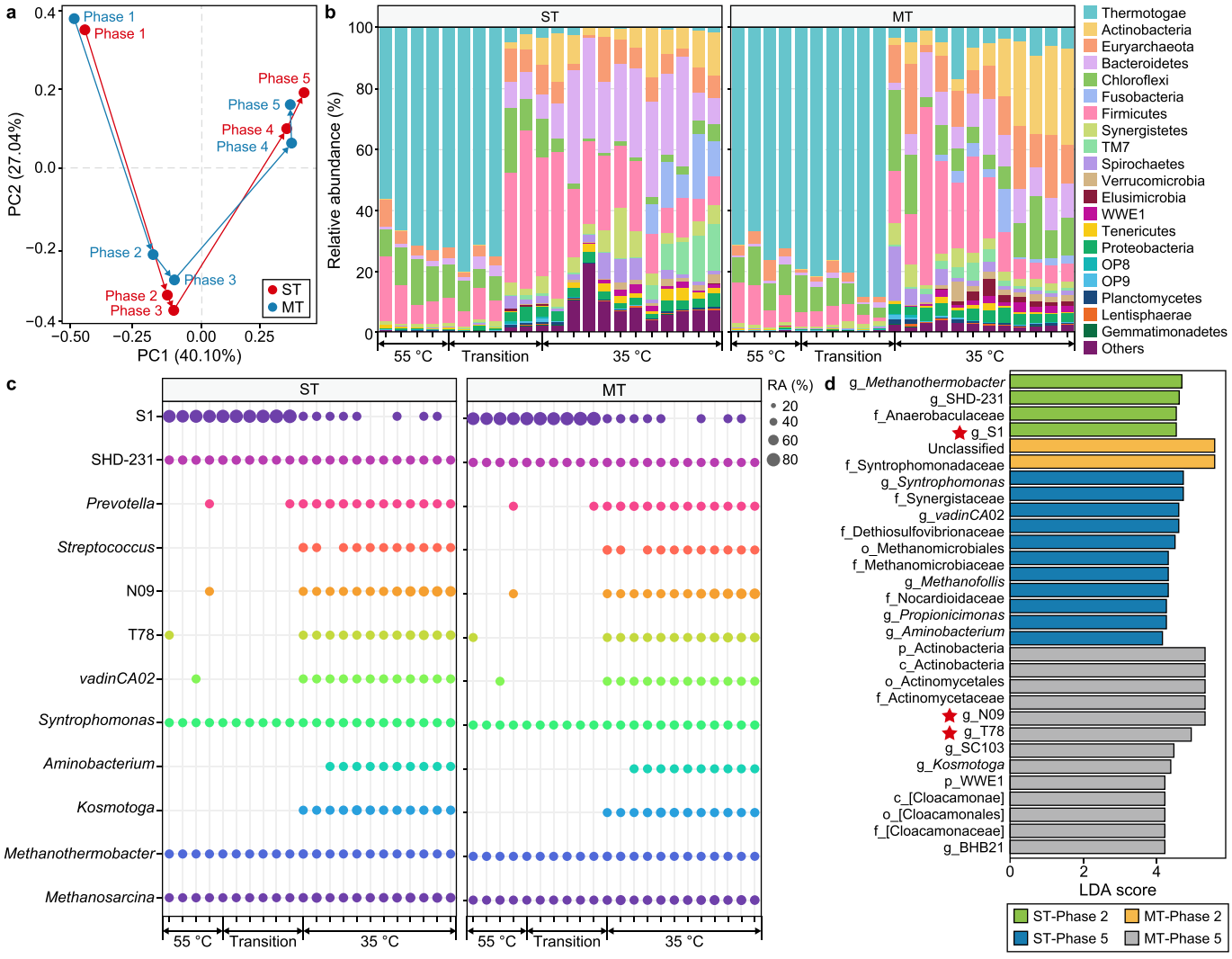

Fig. 4. Microbial dynamics in ST and MT reactors. **a**, PCoA of amplicon sequence variants (ASVs) based on Bray-Curtis distance. **b,** Taxonomy of microbial communities at the phylum level. **c,** Dominant genera in ST and MT. **d,** Cladogram evaluated by LEfSe analysis illustrating the statistically significant taxa in ST and MT with the threshold of LDA score was 2.0 (microbial relative abundance ≥1.0 %).

(2.5–7.9%), *Syntrophomonas* (6.6–7.2%), *vadinCA02* (4.8–6.8%), *Sphaerochaeta* (5.3–5.8%), and N09 (2.2–4.8%) were significantly enriched in ST, while *Kosmotoga* (5.3–6.6%), *Syntrophomonas* (3.4–4.8%), N09 (3.1–3.5%), HA73 (2.2–2.3%), and T78 (2.1–2.2%) predominated in MT. Strikingly, except for *Syntrophomonas*, other functional bacteria serving as mesophiles, were absent in the thermophilic microbiome [21]. Therefore, it can be justifiably speculated that the suitable pH environment facilitated the growth of these immigrant mesophiles from substrates, while the rapid acclimation, colonization, and proliferation of immigrant mesophiles were conducive to performance recovery [34,55]. This might be an important reason for the faster performance recovery in MT. Next, genera N09 (8.6–9.7% in ST, 27.1–29.3% in MT) and T78 (3.7–3.9% in ST, 7.2–10.3% in MT) were taken as biomarkers and became the predominant bacterial groups during phase 5 (Fig. 4d). The increase in the synergistic partners N09 and T78 in MT significantly promoted the abundance and metabolic activities of *Methanosarcina* [56]. The dominance of *Methanosarcina* would benefit the system and produce more CH_4 as the mesophilic conditions favored homoacetogenesis acetate formation [3]. The relative abundance of *Methanosarcina* in MT was 1.5–3.0-fold greater than that in ST, implying that MT was beneficial for better methanogenic performance. Intriguingly, *Methanofollis* (0.8–1.0%) and *Methanobacterium* (1.1–1.7%) were the second most predominant methanogens in ST and MT, respectively. *Methanofollis* grew with CO_2, formate, and ethanol as electron donors to form CH_4 [6] and could be characterized as a strictly mesophilic methanogen, since it was nondetectable in thermophilic conditions. *Methanobacterium* was physiologically recognized as a hydrogenotrophic methanogen capable of producing CH_4 by reducing CO_2 with H_2 or formate as an electron donor [57]. *Methanobacterium* was considered the critical archaeon to recover collapsed cellulose AD systems when the temperature shifted from thermophilic to mesophilic conditions [19]. Thus, the mixotrophic methanogenesis dominated by *Methanosarcina* functioned as the prevalent CH_4 production pathway in steady mesophilic ST and MT reactors. Therefore, the higher abundance of mutualistic bacteria N09 and T78 and mixotrophic methanogens *Methanosarcina* in MT contributed to highly efficient AD performance and the significant production of CH_4. RDA analysis also showed that temperature significantly altered microbial community succession (Supplementary Material Fig. S8), indicating a strong correlation between temperature and microbiome

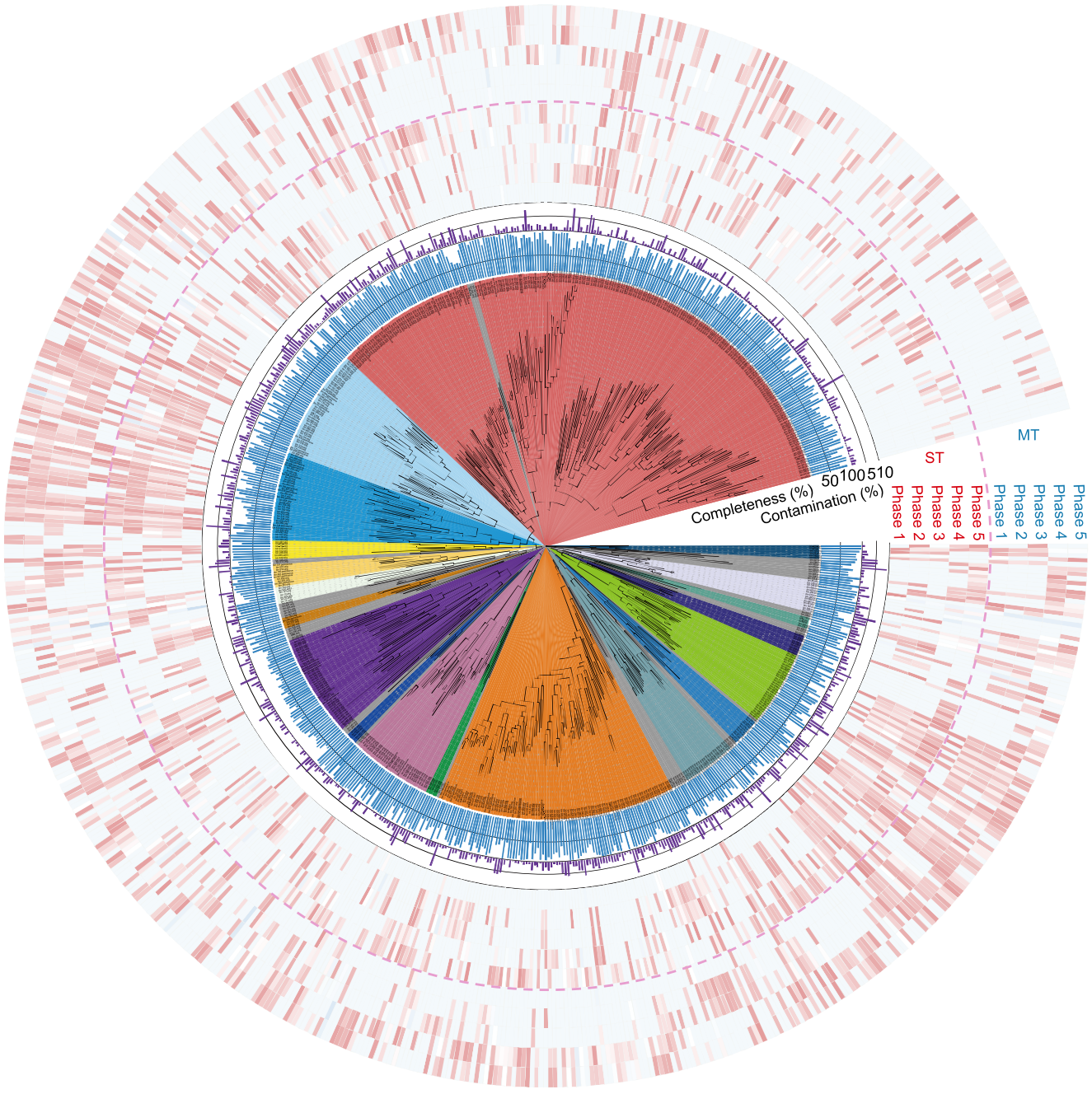

Fig. 5. Phylogenetic genome tree of 695 MAGs. The circle heatmap indicates the relative abundance (%) of MAGs in each phase of the reactors. The bar chart indicates completeness (%) and contamination (%). The inner circle indicates the MAGs' phylum.

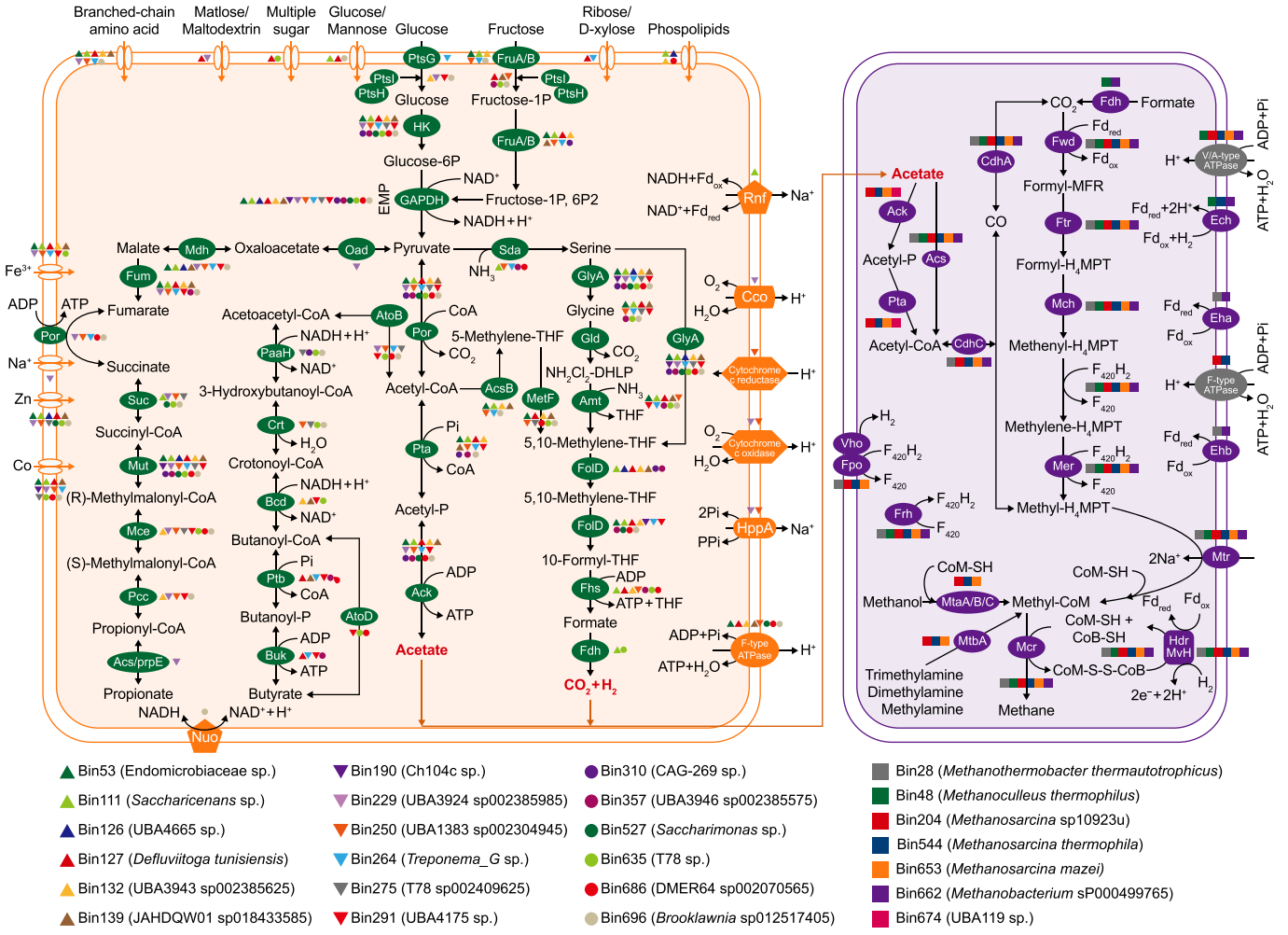

Fig. 6. Metabolic pathway reconstruction of the dominant and functional MAGs recovered from ST and MT microbiomes. The genome annotation was referenced to the KEGG, eggNOG 5.0, dbCAN2, and METABOLIC (v4.0).

structure. In summary, different temperature transition strategies reshaped discrepant microbiota composition, while MT contributed more to enriching core functional microbiomes (N09, T78, *Methanosarcina*), potentially enhancing AD efficiency and CH_4 production.

3.4.2. Functional microbial genomes and their metabolic traits

To further examine key microbial genomes and metabolism mechanisms, 695 dereplicated MAGs were retrieved by metagenomic binning, including 666 bacterial and 29 archaeal genomes (Fig. 5, Supplementary Material Data S1). Specifically, abundant syntrophic acetogens, such as Bin127 (*Defluviitoga tunisiensis*) (39.5–44.7%), Bin229 (UBA3924 sp002385985) (2.9–3.9%), and Bin132 (UBA3943 sp002385625) (2.2–3.1%), were favorably recruited in phase 1. These three MAGs were annotated as important syntrophic acetogens with decarboxylation metabolism (i.e., syntrophic acetate, butyrate, and propionate oxidation), accounting for methanogenic substrate (acetate and CO_2/H_2) production (Fig. 6). The most abundant Bin127 (*Defluviitoga tunisiensis*) was the main contributor to hydrolysis during thermophilic operation [26]. The formed monosaccharides were then biodegraded to acetate through the acetate–ethanol fermentation pathway [48] or to CO_2/H_2 through the conventional syntrophic acetate oxidation (SAO) process. After the ST shift, acidogenic bacteria, such as Bin310 (CAG-269 sp.), Bin139 (JAHDQW01 sp018433585), Bin111 (*Saccharicenans* sp.), Bin190 (Ch104c sp.), and Bin127 (*Defluviitoga tunisiensis*), proliferated and dominated, accounting for 13.3% of microbial communities (Supplementary Material Fig. S9). All these MAGs, other than Bin190 (Ch104c sp.), were genetically capable of acid formation (acetate and butyrate) (Supplementary Material Data S2), while the syntrophic acetogens Bin111 (*Saccharicenans* sp.) and Bin127 (*Defluviitoga tunisiensis*) conducted the conventional SAO process and took up 4.2% of the total relative abundance. Surprisingly, we observed that Bin111 (*Saccharicenans* sp.) contained a complete set of the gene spectrum related to the novel SAO and reductive acetyl-CoA pathway—that is, a glycine cleavage system with a tetrahydrofolate pathway for acetate oxidation to CO_2/H_2 [58]. ST shifted the dominant microbial community from syntrophs to acidogens, resulting in an imbalance of mutualistic microbiota. The dominance of mixotrophic *Methanosarcina* after a temperature shift has been observed in previous studies [44,59], mainly due to the great tolerance of *Methanosarcina* to external environmental stressors, such as temperature fluctuations. In this scenario, the growth of hydrogenotrophic Bin48 (*Methanoculleus thermophilus*) (0.1%) was dramatically suppressed, while acetate-consuming Bin544 (*Methanosarcina thermophila*) (1.9%) obtained slight growth advantages. Despite the enrichment of *M. thermophila*, the high TVFAs in ST (Table 2) reflected a process

imbalance and induced a significant decrease in CH_4 production.

Unlike the dominant ST microbiota in phase 2, MT facilitated the rapid proliferation of acetate-producing bacteria Bin264 (*Treponema_G* sp.) (13.1%), syntrophic propionate oxidation (SPO) bacteria Bin229 (UBA3924 sp002385985) (7.6%), and two SAO bacteria, Bin357 (UBA3946 sp002385575) (3.5%) and Bin111 (*Saccharicenans* sp.) (2.9%). Bin264 (*Treponema_G* sp.) was uniquely found in MT (not observed in ST) and featured as a strictly mesophilic, acid-tolerant acidogen due to its zero abundance in thermophilic digesters and rapid emergence as the most abundant species after the MT shift. Notably, the syntrophic acetogens Bin229 (UBA3924 sp002385985), Bin357 (UBA3946 sp002385575), and Bin111 (*Saccharicenans* sp.) accounted for 14.0% of the total relative abundance and played pivotal roles in decarboxylation metabolisms, thereby alleviating the acidification dominated by acidogen Bin264 (*Treponema_G* sp.). In addition, unlike the rapid substitute behavior in ST, Bin127 (*Defluviitoga tunisiensis*) maintained its dominant role until the end of phase 2 in MT, and the persistence of hydrolytic bacterium Bin127 (*Defluviitoga tunisiensis*) during temperature shift would maintain reactor performance through the generation of acetate and H_2 from monosaccharide degradation [60,61]. Intriguingly, the temperature shifts also caused a shift of dominant methanogens from *M. thermophilus* to *M. thermophila*. Notably, the significantly higher abundance of *M. thermophila* in MT (5.3%) than in ST (1.9%) could further explain the superior performance in MT during temperature transition. This demonstrates that MT facilitated the maintenance of syntrophic interactions within the digestion microcosms during temperature transition and improved the predominant acetoclastic methanogenesis pathway, thereby sustaining robust CH_4 production.

A large variation in mesophilic microbiomes was observed in both ST and MT after performance recovery in phase 5 compared to phase 2. Unexpectedly, the microbial community composition differed significantly between the two reactors, apart from the shared core and predominant member Bin250 (UBA1383 sp002304945). This indicates that, although both reactors recovered by the same pH adjustment, ST and MT still posed different selection pressures on microbial populations. Nevertheless, the differential microbial groups shared highly similar metabolic functions (syntrophic decarboxylation metabolism) in ST and MT. In detail, the function-versatile Bin250 (UBA1383 sp002304945) with genetic capabilities for SAO, SPO, and syntrophic butyrate oxidation (SBO) was favorably enriched in the two reactors. Therefore, a higher abundance of Bin250 (UBA1383 sp002304945) promoted the process of acetogenesis and the formation of methanogenic precursors, which was more favorable for CH_4 production. This partially explains the greater methanogenic performance of MT over ST during steady mesophilic operation given the significantly higher population of Bin250 (UBA1383 sp002304945) in MT (13.7%) than in ST (5.0%). Intriguingly, the dominant methanogen varied in ST but retained in MT during stable mesophilic operation, implying that the two reactors selectively enriched their dominant methanogens. For example, the most abundant archaeon, Bin653 (*Methanosarcina mazei*) (2.2%) instead of *M. thermophila* (1.4%), was determined in ST microbiomes, which incorporated genes for acetoclastic, hydrogenotrophic, and methylotrophic methanogenic pathways. *M. mazei* has previously been identified as participating in direct interspecies electron transfer (DIET) [62,63] and performing electromethanogenesis under limited electron-transfer mediators, such as H_2 or formate [64]. Nevertheless, typical electroactive bacteria (i.e., *Geobacter*) were not detected in the mesophilic microbiota, suggesting that other methanogenic substrates may promote the growth of the dominant *M. mazei*. Considering the dominance of acetate-producing members in ST (i.e., Bin527 (*Saccharimonas* sp.) and Bin696 (*Brooklawnia* sp012517405)) and the high affinity of *M. mazei* for acetate, as previously documented [63], we can infer that *M. mazei* preferentially utilizes acetate for CH_4 formation and assign its functional role as an acetoclastic methanogen. Additionally, acetoclastic *M. thermophila* (4.8%) maintained dominance in the archaeal community throughout the stable mesophilic operation of MT. These findings reveal that temperature transition altered the trophic-level patterns of methanogens—for example, from hydrogenotrophic to acetoclastic methanogenesis—to scavenge methanogenic substrate, which is acetate derived from the prevalent acetate-forming and homoacetogenesis pathways in mesophilic conditions [3,65]. Moreover, MT (4.8%) constituted a higher abundance of acetoclastic methanogens than ST (3.6%), demonstrating that MT manipulated more efficient acetate degradation to generate CH_4. Overall, multiple functional members of acid-producing bacteria; syntrophs involved in SAO, SPO, and SBO; and acetoclastic methanogens collaborated in mesophilic microbiomes, while with greater members in MT, more robust and efficient CH_4 generation was performed.

3.4.3. Microbial interaction networks

To better interpret the microbial ecological interactions within the AD microbiome subjected to temperature shift, a co-occurrence network analysis of MAGs was conducted. In the complex AD microcosm, different microbial species, represented by nodes, interact with each other through the flow of information, materials, and energy to curate a vast and complex ecological network [66]. The network composition was remarkably different between ST and MT in phase 2, as reflected in the two ecological networks of different sizes for ST (350 nodes) and MT (193 nodes) that were constructed (Supplementary Material Fig. S10). Meanwhile, the significantly higher total edges and degree distributions were enhanced after temperature shift, thereby elevating microbial functional redundancy. Notably, the shift in node links toward the single nodes in the modules elucidated the possible movement of the network structure toward an imbalance in microbiome functionality [67]. The imbalance in microbial interactions and increase in species competition resulted in decreased metabolic and biomass accumulation rates under a temperature drop [68], thereby causing microbial syntrophic interaction loss and a significant decline in CH_4 productivity for ST in phase 2 [66]. Network modularity indicates niche or functional units in the microbial community and represents community stability and robustness [8,65]. Higher modularity is typically associated with highly functional microbial networks, more complex interspecies interactions, and higher resistance against environmental stresses [2,66]. However, given the lower CH_4 production in phase 2 of ST, the higher modularity index (0.658) may be a consequence of redundant anaerobes' colonization (i.e., Bin310 (CAG-269 sp.) and Bin139 (JAHDQW01 sp018433585)), which considerably reduced the efficiency of the conversion of organics to CH_4 due to the loss of core and functional pathways. In addition, ST-induced excessive ROS may disrupt genetic integrity and impede the transcription of genes, leading to the dysfunction of essential microbial metabolism [69]. Compared with ST in phase 2, MT exhibited fewer nodes, edge numbers, degrees, and modularity, indicating that it had less complex microbial interaction types than ST. The lower modularity in MT (0.579) can be ascribed to (i) the centralization of functional pathways by the abundant thermophiles [49] and (ii) microbial adaptation within the ecosystem to establish suitable niches and functional units [8]. Previous studies have confirmed that high temperature reduces network modularity and microbial biodiversity, forming central functional pathways in AD [8,49], which help

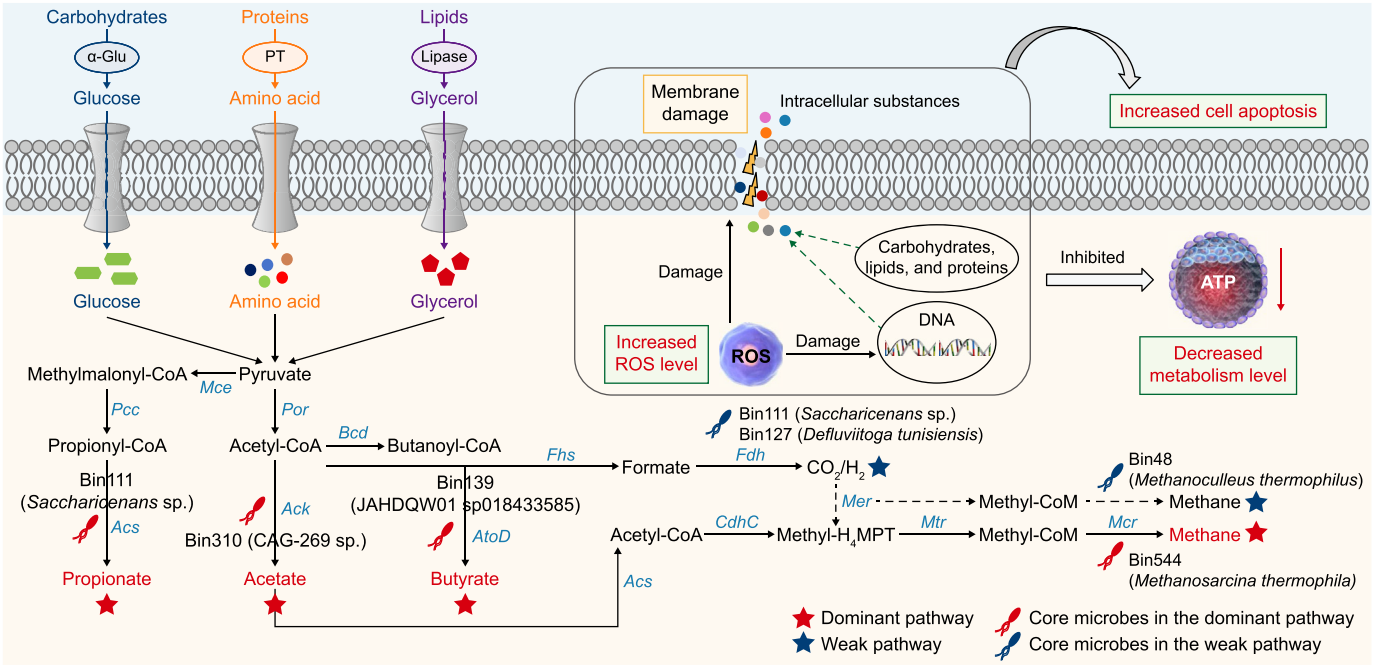

Fig. 7. Schematic diagram of sharp temperature shift stress on AcoD of WAS with FW and the resulting cellular metabolism mechanisms. ROS: reactive oxygen species.

maintain necessary system functioning and process stability during MT.

Furthermore, the observed higher CH_4 production operated by MT can be illustrated by the co-occurrence network interactions in which the rapid acclimation and colonization of microbial populations linked more species into complex subunits (modules) and correspondingly raised interconnections within major modules [8], indicated by a decline in modularity (0.435) and an increase in average degrees (44.9). Such characteristics manifested in MT increased interspecies interactions and essential functional modules and, thus, led to more efficient methanogenetic syntrophy. Hence, maintaining and enhancing microbial interconnections is essential to relieve the side effects of temperature-dependent functional diminution and gain contact supremacy between syntrophs and methanogens [6].

3.5. Mechanisms of temperature decline stress on thermophilic microbes

Temperature is a crucial operational factor in determining system performance and stability, influencing cell physiology and altering microbial communities, functional traits, and interspecies interactions [3,13]. Transforming AcoD from thermophilic to mesophilic conditions displayed different negative impacts on overall performance via ST and MT strategies. The temperature transition using MT resulted in a 38.9% decrease in CH_4 production, which was significantly lower than when using ST (88.8% decrease). The relatively higher stable performance in MT can be attributed to the persistence of thermophiles (Bin127 (*Defluviitoga tunisiensis*)) in the mild hypothermic state. In contrast, ST caused a serious deterioration of reactor performance due to the high sensitivity of thermophiles to violent temperature variations [13]. Combining metagenomic analysis and biochemical and molecular approaches, a mechanistic model of the ST-influenced ecosystem is proposed (Fig. 7). Specifically, the intense oxidative stress caused by ROS overproduction in ST can be inferred as the primary cause of the system breakdown, which immensely damaged the membrane permeability and integrity and downregulated the cell metabolism level, triggering an increase in the apoptosis of anaerobes and excessive release of intracellular substances. Subsequently, ST directly reshaped microbial community assembly patterns and dramatically altered the metabolic functions of the community. The acidogens outcompeted slow-growing syntrophic bacteria and methanogens and overgrew through uptaking the rich substrates (glucose, glycerol, cellobiose, and amino acids) that stemmed from vigorous hydrolyzers. The prevalent genomes attributed to acidogenic bacteria significantly simplified complex syntrophic interactions. They gave rise to an imbalance in microbiome functionality, substantially reducing the expression level of key enzymes associated with acidogenesis, acetogenesis, and methanogenesis processes. Therefore, a dramatic temperature shift conspicuously inhibited the growth of most microbes in AD ecosystems and substantially reduced CH_4 production. Notably, MT was demonstrated to be effective in relieving temperature decline stress on cell viability and normal metabolism during temperature transition. Furthermore, MT performed better than ST during stable operation, with an increased abundance of functional microbes, enhanced interspecies interactions, and improved metabolic activities. We recommend MT as a feasible solution for reforming the existing thermophilic digesters to mesophilic ones, offering a roadmap for engineered systems toward more robust, efficient, flexible, and extensive applications.

4. Conclusion

The present study demonstrated that a mild temperature transition is a valid approach for transforming thermophilic digesters into mesophilic digesters during the AcoD of WAS with FW. In contrast to MT, ST substantially reduced CH_4 production by inducing high oxidative stress and, thus, significantly disrupting membrane permeability, attenuating metabolic activity, and increasing cell lysis and the leakage of intracellular substances. Moreover, ST destroyed the microbial interaction network and triggered the loss of key functional modules associated with CH_4

production. This led to a significant decline in metabolic capability at the organic, enzyme, and gene levels in methanogenesis. In contrast, MT facilitated the enrichment of immigrant mesophiles, increased the abundance of key syntrophs, boosted crucial CH_4 generation processes, and enabled the higher expression of acetate-dependent methanogenesis genes, resulting in improved and efficient methanogenic performance during stable mesophilic operation. Overall, this study provides a holistic understanding of the effects of temperature shifts on thermophilic digestion and extends the application scenarios of AD to various seasons and regions.

CRediT authorship contribution statement

Xingxing Zhang: Data Curation, Investigation, Methodology, Writing - Original Draft. **Pengbo Jiao:** Investigation. **Yiwei Wang:** Investigation. **Yinying Dai:** Investigation. **Ming Zhang:** Formal Analysis, Writing - Review & Editing. **Peng Wu:** Formal Analysis, Writing - Review & Editing. **Liping Ma:** Conceptualization, Formal Analysis, Writing - Review & Editing.

Declaration of competing interest

The authors declare that they have no known competing financial interests or personal relationships that could have appeared to influence the work reported in this paper.

Acknowledgements

This study was financially supported by the National Key Research and Development Program of China (2019YFC1905001), the National Natural Science Foundation of China (41907356), and the Program for Professor of Special Appointment (Eastern Scholar) (TP2019020).

Appendix A. Supplementary data

Supplementary data to this article can be found online at https://doi.org/10.1016/j.ese.2024.100440.

References

[1] L. Sillero, R. Solera, M. Pérez, Thermophilic-mesophilic temperature phase anaerobic co-digestion of sewage sludge, wine vinasse and poultry manure: effect of hydraulic retention time on mesophilic-methanogenic stage, Chem. Eng. J. 451 (2023) 138478.
[2] M. Jiang, P. Wang, H. Liu, X. Dai, S. Song, Y. Liu, The effect of operating strategies on the anaerobic digestion of gentamicin mycelial residues: insights into the enhancement of methane production and attenuation of gentamicin resistance, Environ. Sci. Technol. 56 (21) (2022) 15130–15140.
[3] E. Nie, P. He, H. Zhang, L. Hao, L. Shao, F. Lü, How does temperature regulate anaerobic digestion? Renew. Sust. Energ. Rev. 150 (2021) 111453.
[4] J. Kim, C. Lee, Response of a continuous anaerobic digester to temperature transitions: a critical range for restructuring the microbial community structure and function, Water Res. 89 (2016) 241–251.
[5] H. Yun, B. Liang, Y. Ding, S. Li, Z. Wang, A. Khan, P. Zhang, P. Zhang, A. Zhou, A. Wang, X. Li, Fate of antibiotic resistance genes during temperature-changed psychrophilic anaerobic digestion of municipal sludge, Water Res. 194 (2021) 116926.
[6] X. Zhang, Y. Wang, P. Jiao, M. Zhang, Y. Deng, C. Jiang, X.-W. Liu, L. Lou, Y. Li, X.-X. Zhang, L. Ma, Microbiome-functionality in anaerobic digesters: a critical review, Water Res. 249 (2024) 120891.
[7] U. Tezel, M. Tandukar, M.G. Hajaya, S.G. Pavlostathis, Transition of municipal sludge anaerobic digestion from mesophilic to thermophilic and long-term performance evaluation, Bioresour. Technol. 170 (2014) 385–394.
[8] Z. Lv, P. Lyu, K. Li, F. Song, Z. Zhang, Y. Yang, H. Yu, High temperature shock threatens methane production via disturbing microbial interactions in anaerobic digestion, Sci. Total. Environ. 846 (2022) 157459.
[9] J. Shin, H.M. Jang, S.G. Shin, Y.M. Kim, Thermophilic anaerobic digestion: effect of start-up strategies on performance and microbial community, Sci. Total. Environ. 687 (2019) 87–95.
[10] H.M. Jang, J.H. Ha, M.S. Kim, J.O. Kim, Y.M. Kim, J.M. Park, Effect of increased load of high-strength food wastewater in thermophilic and mesophilic anaerobic co-digestion of waste activated sludge on bacterial community structure, Water Res. 99 (2016) 140–148.
[11] M. Kumar, S. Dutta, S. You, G. Luo, S. Zhang, P.L. Show, A.D. Sawarkar, L. Singh, D.C.W. Tsang, A critical review on biochar for enhancing biogas production from anaerobic digestion of food waste and sludge, J. Clean. Prod. 305 (2021) 127143.
[12] A. Iqbal, F. Zan, M.A. Siddiqui, S. Nizamuddin, G. Chen, Integrated treatment of food waste with wastewater and sewage sludge: energy and carbon footprint analysis with economic implications, Sci. Total. Environ. 825 (2022) 154052.
[13] S. Hupfauf, P. Plattner, A.O. Wagner, R. Kaufmann, H. Insam, S.M. Podmirseg, Temperature shapes the microbiota in anaerobic digestion and drives efficiency to a maximum at 45 degrees C, Bioresour. Technol. 269 (2018) 309–318.
[14] Q. Xu, S. Long, X. Liu, A. Duan, M. Du, Q. Lu, L. Leng, S.Y. Leu, D. Wang, Insights into the occurrence, fate, impacts, and control of food additives in food waste anaerobic digestion: a review, Environ. Sci. Technol. 57 (17) (2023) 6761–6775.
[15] L. Tian, H. Guo, Y. Wang, J. Hou, T. Zhu, Y. Tong, P. Sun, Y. Liu, Unveiling the mechanism of urine source separation-derived pretreatment on enhancing short-chain fatty acid yields from anaerobic fermentation of waste activated sludge, Environ. Sci. Technol. 56 (22) (2022) 16178–16188.
[16] J. Li, X. Ran, M. Zhou, K. Wang, H. Wang, Y. Wang, Oxidative stress and antioxidant mechanisms of obligate anaerobes involved in biological waste treatment processes: a review, Sci. Total. Environ. 838 (Pt 3) (2022) 156454.
[17] J. Wang, D. Ma, K. Feng, Y. Lou, H. Zhou, B. Liu, G. Xie, N. Ren, D. Xing, Polystyrene nanoplastics shape microbiome and functional metabolism in anaerobic digestion, Water Res. 219 (2022) 118606.
[18] C. Liu, H. Wang, M. Usman, M. Ji, J. Sha, Z. Liang, L. Zhu, L. Zhou, B. Yan, Nonmonotonic effect of CuO nanoparticles on medium-chain carboxylates production from waste activated sludge, Water Res. 230 (2023) 119545.
[19] C. Madigou, K.-A. Lê Cao, C. Bureau, L. Mazéas, S. Déjean, O. Chapleur, Ecological consequences of abrupt temperature changes in anaerobic digesters, Chem. Eng. J. 361 (2019) 266–277.
[20] G. Luo, D. De Francisci, P.G. Kougias, T. Laura, X. Zhu, I. Angelidaki, New steady-state microbial community compositions and process performances in biogas reactors induced by temperature disturbances, Biotechnol. Biofuels. 8 (2015) 3.
[21] K. Hagos, J. Zong, D. Li, C. Liu, X. Lu, Anaerobic co-digestion process for biogas production: progress, challenges and perspectives, Renew. Sust. Energ. Rev. 76 (2017) 1485–1496.
[22] P.N. Evans, J.A. Boyd, A.O. Leu, B.J. Woodcroft, D.H. Parks, P. Hugenholtz, G.W. Tyson, An evolving view of methane metabolism in the Archaea, Nat. Rev. Microbiol. 17 (4) (2019) 219–232.
[23] J.U. Kreft, B.M. Griffin, R. Gonzalez-Cabaleiro, Evolutionary causes and consequences of metabolic division of labour: why anaerobes do and aerobes don't, Curr. Opin. Biotechnol. 62 (2020) 80–87.
[24] A. Detman, D. Laubitz, A. Chojnacka, P.R. Kiela, A. Salamon, A. Barberan, Y. Chen, F. Yang, M.K. Blaszczyk, A. Sikora, Dynamics of dark fermentation microbial communities in the light of lactate and butyrate production, Microbiome 9 (1) (2021) 158.
[25] Y. Chen, Q. Ping, D. Li, X. Dai, Y. Li, Comprehensive insights into the impact of pretreatment on anaerobic digestion of waste active sludge from perspectives of organic matter composition, thermodynamics, and multi-omics, Water Res. 226 (2022) 119240.
[26] C. Wang, Y. Wang, Y. Wang, L. Liu, D. Wang, F. Ju, Y. Xia, T. Zhang, Impacts of food waste to sludge ratios on microbial dynamics and functional traits in thermophilic digesters, Water Res. 219 (2022) 118590.
[27] C. Wang, J. Liu, X. Xu, L. Zhu, Response of methanogenic granules enhanced by magnetite to ammonia stress, Water Res. 212 (2022) 118123.
[28] X. Zhang, P. Jiao, Y. Wang, P. Wu, Y. Li, L. Ma, Enhancing methane production in anaerobic co-digestion of sewage sludge and food waste by regulating organic loading rate, Bioresour. Technol. 363 (2022) 127988.
[29] H. Wang, H. Sun, H. Ren, G. Cao, G. Xie, D. Xing, N. Ren, B. Liu, Metagenomic reveals the methanogenesis metabolic mechanism of high-solids anaerobic digestion of human feces under gradient domestication, Chem. Eng. J. 460 (2023) 141752.
[30] G.A.W. Sudiartha, T. Imai, C. Mamimin, A. Reungsang, Effects of temperature shifts on microbial communities and biogas production: an in-depth comparison, Fermentation 9 (7) (2023) 642.
[31] J. De Vrieze, M. De Waele, P. Boeckx, N. Boon, Isotope fractionation in biogas allows direct microbial community stability monitoring in anaerobic digestion, Environ. Sci. Technol. 52 (11) (2018) 6704–6713.
[32] W. Zhang, L. Li, W. Xing, B. Chen, L. Zhang, A. Li, R. Li, T. Yang, Dynamic behaviors of batch anaerobic systems of food waste for methane production under different organic loads, substrate to inoculum ratios and initial pH, J. Biosci. Bioeng. 128 (6) (2019) 733–743.
[33] X. Dai, X. Li, D. Zhang, Y. Chen, L. Dai, Simultaneous enhancement of methane production and methane content in biogas from waste activated sludge and perennial ryegrass anaerobic co-digestion: the effects of pH and C/N ratio, Bioresour. Technol. 216 (2016) 323–330.
[34] R. Mei, W.T. Liu, Meta-omics-supervised characterization of respiration activities associated with microbial immigrants in anaerobic sludge digesters, Environ. Sci. Technol. 56 (10) (2022) 6689–6698.
[35] N.M. Coelho, R.L. Droste, K.J. Kennedy, Evaluation of continuous mesophilic, thermophilic and temperature phased anaerobic digestion of microwaved

activated sludge, Water Res. 45 (9) (2011) 2822–2834.
[36] P. Izadi, P. Izadi, A. Eldyasti, Holistic insights into extracellular polymeric substance (EPS) in anammosx bacterial matrix and the potential sustainable biopolymer recovery: a review, Chemosphere 274 (2021) 129703.
[37] G.-F. Li, B.-C. Huang, Y.-F. Cheng, W.-J. Ma, S.-T. Li, B. Gong, Y.-F. Guan, N.-S. Fan, R.-C. Jin, Determination of the response characteristics of anaerobic ammonium oxidation bioreactor disturbed by temperature change with the spectral fingerprint, Sci. Total. Environ. 719 (2020) 137513.
[38] J. De Vrieze, A.M. Saunders, Y. He, J. Fang, P.H. Nielsen, W. Verstraete, N. Boon, Ammonia and temperature determine potential clustering in the anaerobic digestion microbiome, Water Res. 75 (2015) 312–323.
[39] H. Chen, S. Chang, Dissecting methanogenesis for temperature-phased anaerobic digestion: impact of temperature on community structure, correlation, and fate of methanogens, Bioresour. Technol. 306 (2020) 123104.
[40] J.B. Fellman, E. Hood, R.G.M. Spencer, Fluorescence spectroscopy opens new windows into dissolved organic matter dynamics in freshwater ecosystems: a review, Limnol. Oceanogr. 55 (6) (2010) 2452–2462.
[41] Y. Li, X. Li, P. Wang, Y. Su, B. Xie, Size-dependent effects of polystyrene microplastics on anaerobic digestion performance of food waste: focusing on oxidative stress, microbial community, key metabolic functions, J. Hazard. Mater. 438 (2022) 129493.
[42] X. Lin, Y. Wang, X. Ma, Y. Yan, M. Wu, P.L. Bond, J. Guo, Evidence of differential adaptation to decreased temperature by anammox bacteria, Environ. Microbiol. 20 (10) (2018) 3514–3528.
[43] M. Khademian, J.A. Imlay, How microbes evolved to tolerate oxygen, Trends Microbiol. 29 (5) (2021) 428–440.
[44] Z. Wu, D. Nguyen, T.Y.C. Lam, H. Zhuang, S. Shrestha, L. Raskin, S.K. Khanal, P.H. Lee, Synergistic association between cytochrome bd-encoded Proteiniphilum and reactive oxygen species (ROS)-scavenging methanogens in microaerobic-anaerobic digestion of lignocellulosic biomass, Water Res. 190 (2021) 116721.
[45] W. Wei, Y.T. Zhang, Q.S. Huang, B.J. Ni, Polyethylene terephthalate microplastics affect hydrogen production from alkaline anaerobic fermentation of waste activated sludge through altering viability and activity of anaerobic microorganisms, Water Res. 163 (2019) 114881.
[46] X. Liu, Q. Lu, M. Du, Q. Xu, D. Wang, Hormesis-like effects of tetrabromobisphenol A on anaerobic digestion: responses of metabolic activity and microbial community, Environ. Sci. Technol. 56 (16) (2022) 11277–11287.
[47] M. Du, X. Liu, D. Wang, Q. Yang, A. Duan, H. Chen, Y. Liu, Q. Wang, B.J. Ni, Understanding the fate and impact of capsaicin in anaerobic co-digestion of food waste and waste activated sludge, Water Res. 188 (2021) 116539.
[48] H. Zhang, W. Yuan, Q. Dong, D. Wu, P. Yang, Y. Peng, L. Li, X. Peng, Integrated multi-omics analyses reveal the key microbial phylotypes affecting anaerobic digestion performance under ammonia stress, Water Res. 213 (2022) 118152.
[49] Q. Lin, J. De Vrieze, G. He, X. Li, J. Li, Temperature regulates methane production through the function centralization of microbial community in anaerobic digestion, Bioresour. Technol. 216 (2016) 150–158.
[50] Y. Li, X. Zhang, H. Xu, H. Mu, D. Hua, F. Jin, G. Meng, Acidogenic properties of carbohydrate-rich wasted potato and microbial community analysis: effect of pH, J. Biosci. Bioeng. 128 (1) (2019) 50–55.
[51] A. Ajayi-Banji, S. Rahman, A review of process parameters influence in solid-state anaerobic digestion: focus on performance stability thresholds, Renew. Sust. Energ. Rev. 167 (2022) 112756.
[52] W. Du, F. Wang, S. Fang, W. Huang, X. Cheng, J. Cao, F. Fang, Y. Wu, J. Luo, Antimicrobial PCMX facilitates the volatile fatty acids production during sludge anaerobic fermentation: insights of the interactive principles, microbial metabolic profiles and adaptation mechanisms, Chem. Eng. J. 446 (2022) 137339.
[53] M. Jiang, W. Qiao, Y. Wang, T. Zou, M. Lin, R. Dong, Balancing acidogenesis and methanogenesis metabolism in thermophilic anaerobic digestion of food waste under a high loading rate, Sci. Total. Environ. 824 (2022) 153867.
[54] Y. Li, J. Ni, H. Cheng, A. Zhu, G. Guo, Y. Qin, Y.Y. Li, Methanogenic performance and microbial community during thermophilic digestion of food waste and sewage sludge in a high-solid anaerobic membrane bioreactor, Bioresour. Technol. 342 (2021) 125938.
[55] R. Montañés, M. Pérez, R. Solera, Anaerobic mesophilic co-digestion of sewage sludge and sugar beet pulp lixiviation in batch reactors: effect of pH control, Chem. Eng. J. 255 (2014) 492–499.
[56] M. Gao, B. Guo, L. Li, Y. Liu, Role of syntrophic acetate oxidation and hydrogenotrophic methanogenesis in co-digestion of blackwater with food waste, J. Clean. Prod. 283 (2021) 125393.
[57] W. Li, Y. Liu, B. Wu, L. Gu, R. Deng, Upgrade the high-load anaerobic digestion and relieve acid stress through the strategy of side-stream micro-aeration: biochemical performances, microbial response and intrinsic mechanisms, Water Res. 221 (2022) 118850.
[58] L. Hao, T.Y. Michaelsen, C.M. Singleton, G. Dottorini, R.H. Kirkegaard, M. Albertsen, P.H. Nielsen, M.S. Dueholm, Novel syntrophic bacteria in full-scale anaerobic digesters revealed by genome-centric metatranscriptomics, ISME J. 14 (4) (2020) 906–918.
[59] Z. Tian, Y. Zhang, Y. Li, Y. Chi, M. Yang, Rapid establishment of thermophilic anaerobic microbial community during the one-step startup of thermophilic anaerobic digestion from a mesophilic digester, Water Res. 69 (2015) 9–19.
[60] D. Wu, L. Li, F. Zhen, H. Liu, F. Xiao, Y. Sun, X. Peng, Y. Li, X. Wang, Thermodynamics of volatile fatty acid degradation during anaerobic digestion under organic overload stress: the potential to better identify process stability, Water Res. 214 (2022) 118187.
[61] S. Campanaro, L. Treu, P.G. Kougias, G. Luo, I. Angelidaki, Metagenomic binning reveals the functional roles of core abundant microorganisms in twelve full-scale biogas plants, Water Res. 140 (2018) 123–134.
[62] E. Quispe-Cardenas, S. Rogers, Microbial adaptation and response to high ammonia concentrations and precipitates during anaerobic digestion under psychrophilic and mesophilic conditions, Water Res. 204 (2021) 117596.
[63] F. Liu, S. Zheng, B. Wang, X. Zhang, Selectively facilitating the electron acceptance of methanogens by riboflavin, Renew. Energ. 195 (2022) 734–741.
[64] Y. Yan, J. Zhang, L. Tian, X. Yan, L. Du, A. Leininger, M. Zhang, N. Li, Z.J. Ren, X. Wang, DIET-like mutualism of *Geobacter* and methanogens at specific electrode potential boosts production of both methane and hydrogen from propionate, Water Res. 235 (2023) 119911.
[65] F. Ju, F. Lau, T. Zhang, Linking microbial community, environmental variables, and methanogenesis in anaerobic biogas digesters of chemically enhanced primary treatment sludge, Environ. Sci. Technol. 51 (7) (2017) 3982–3992.
[66] Q. Lu, D. He, X. Liu, M. Du, Q. Xu, D. Wang, 1-Butyl-3-methylimidazolium chloride affects anaerobic digestion through altering organics transformation, cell viability, and microbial community, Environ. Sci. Technol. 57 (8) (2023) 3145–3155.
[67] J.V. Mercado, M. Koyama, K. Nakasaki, Co-occurrence network analysis reveals loss of microbial interactions in anaerobic digester subjected to repeated organic load shocks, Water Res. 221 (2022) 118754.
[68] F.C. García, T. Clegg, D.B. O'Neill, R. Warfield, S. Pawar, G. Yvon-Durocher, The temperature dependence of microbial community respiration is amplified by changes in species interactions, Nat. Microbiol. 8 (2) (2023) 272–283.
[69] S. Huang, B. Zhang, Z. Zhao, C. Yang, B. Zhang, F. Cui, P.N.L. Lens, W. Shi, Metagenomic analysis reveals the responses of microbial communities and nitrogen metabolic pathways to polystyrene micro(nano)plastics in activated sludge systems, Water Res. 241 (2023) 120161.